The Removal of Transients from OTH Radar Signals Via Wavelets

S. E. Godfrey
High Frequency Radar Division
Defence Science and Technology Organisation
Salisbury, South Australia, 5108

Abstract

In skywave radar the removal of transients from the signal is a major objective since they reduce the radar's capability to detect and track targets. It is desirable to extract the transient components from the data without removing any other information. Current techniques only exploit the time localization of such signals. A natural extension would be to incorporate a frequency localization component. Wavelets lend themselves ideally to this task by virtue of their joint time and frequency localization properties. In this paper, we construct a multiresolution wavelet decomposition algorithm for HF radar data and apply two filtering techniques specifically designed to detect and remove lightning and meteor components from the signal.

1 Introduction

OTH (Over-the-Horizon) radar involves transmitting and receiving high frequency (HF) signals via the ionosphere. The received data contains terrestial, environmental and target information from a particular region. The presence of transients in the data due to meteor echoes and lightning bursts affect the ability of the radar to detect targets because of the resultant spread in Doppler (frequency) and the increase in the noise floor. Therefore, the removal of transients is a major concern in OTH radar [1, 2, 3].

Currently, transients are detected in either the time or Doppler domain by locating samples which exhibit energy above a particular threshold. The samples are removed from the data and replaced by interpolation between the remaining data points. The effects of this however, can degrade the non-transient information such as ground clutter and targets. For example, if the transient existed for a good portion of the time series, (technically it is no longer a transient, but we consider a signal that exists for less than the full observation time in this class), the remaining data would not produce a reliable interpolation over the affected time interval. Hence, desired target returns could be degraded or lost. Our aim is to apply a technique which minimizes the disruption to the non-transient information when excising the transient component from the data.

An ideal tool for such a task is wavelets. The joint time and frequency localization properties of the wavelet transform provides a representation of the data such that the transient can be identified by theses two characteristics. The excision process can then be isolated to this time-frequency subspace.

The paper is organised as follows. In Section 2 we present a brief description of the wavelet decomposition algorithm which is used in this analysis. In Section 3 we address a number of considerations when applying wavelet theory to HF radar data obtained from the Australian Jindalee OTH radar. This leads to the construction of two filtering operations aimed at the removal of transient signals in the data. In section 4 we apply these techniques to OTH radar data which contain lightning and meteor echos. The success of each process is indicated by the extent of transient suppression and target preservation in the reconstructed data. Finally, in Section 5 we deduce some conclusions on the applicability of wavelets to our data and discuss extensions to the techniques.

2 Wavelet decomposition — theory

The wavelet transform is a time-scale representation of a signal with respect to the translations and dilations of a wavelet function. In contrast to the Fourier transform, these basis functions are localized in both time and frequency. Furthermore, wavelets are not restricted to a single function type, therefore, they may be chosen (within certain guidelines) to match a specific characteristic in the data. The transformation is linear, so the distribution does not suffer from cross-terms as is the case for quadratic time-frequency distributions such as the Cohen-class. A further advantage is that it enables an analysis of data at multiple levels of resolution.

In the case of discrete data, the decomposition can be carried out via what is known as a *multiresolution wavelet decomposition*, [4, 5]. We include a brief description of the algorithm as followed by our processing.

A set of subspaces $\{V_j\}_{j\in Z}$ is a multiresolution approximation of $L^2(R)$ if it possesses the following properties:

$$V_j \subset V_{j+1} \qquad \forall j \in Z$$

$$\bigcup_{j\in Z} V_j \quad \text{is dense in } L^2(R)$$

$$\bigcap_{j\in Z} V_j = \emptyset$$

$$f(x) \in V_j \Leftrightarrow f(2x) \in V_{j+1} \qquad \forall j \in Z$$

$$f(x) \in V_j \Leftrightarrow f(x - 2^{-j}i) \in V_j \quad \forall j, i \in Z$$

Consider the function $\phi(x)$, which is called a scaling function. It satisfies the dilation equation $\phi(x) = \sum_k c_k \phi(2x - k)$ where c_k are the scaling function coefficients, and has a low-pass filter Fourier transform $\Phi(\omega)$ satisfying $|\Phi(\omega)| \leq 1$ and $|\Phi(0)| = 1$. The translations and dilations of this function produce an orthonormal family $\{\phi_{ij}\}_{ij \in Z} = \{2^{j/2}\phi(2^j x - i)\}_{ij \in Z}$ which generate the subspaces $\{V_j\}_{j \in Z}$. An approximation of a function $f(x) \in L^2(R)$ at resolution 2^{-J} can then be defined as the projection

$$A_J f(x) = \sum_i a_i^J \phi_{iJ}(x) \qquad \in V_J \ ,$$

where $a_i^J = \langle f, \phi_{iJ} \rangle$ is the inner product of the function with the scaling function at scale J and position i. These *expansion coefficients* capture the information in the signal at this resolution level.

On projection from a fine to a coarser scale, some information is lost, namely the details in $f(x)$ that are finer in resolution than 2^{-J}. There exists a subspace W_j which is the orthogonal complement of V_j in V_{j+1} such that $V_j \bigoplus W_j = V_{j+1}$. The subspace W_j is spanned by the orthogonal basis functions $\{\psi_{ij}\}_{i \in Z} = \{2^{j/2}\psi(2^j x - i)\}_{i \in Z}$, where $\psi(x)$ is the wavelet function and the set $\{\psi_{ij}\}_{ij \in Z}$ is an orthogonal basis for $L^2(R)$. Therefore,

$$A_{J+1} f(x) = A_J f(x) + D_J f(x) \ ,$$

where

$$D_J f(x) = \sum_i d_i^J \psi_{iJ}(x)$$

and $d_i^j = \langle f, \psi_{ij} \rangle$ are the *wavelet coefficients* which contain the detail in the signal lost in going from resolution 2^{-j} to $2^{-(j+1)}$. By iteration,

$$\begin{aligned} A_{J+1} f(x) &= D_J f(x) + D_{J-1} f(x) + \cdots \\ &\quad \cdots + D_{J-K} f(x) + A_{J-K} f(x) \ , \end{aligned}$$

where $D_J f(x)$ contains the finest detail and $D_{J-K} f(x)$ and $A_{J-K} f(x)$ which contain the coarsest resolution detail and approximation, respectively.

For measured (finite) data, the finest resolution is limited to $2^0 = 1$. Hence the decomposition is of the form

$$\begin{aligned} f(x) &= A_0 f(x) \\ &= D_{-1} f(x) + D_{-2} f(x) + \quad \cdots \\ &\quad \cdots + D_{-m} f(x) + A_{-m} f(x) \end{aligned}$$

where $N = 2^m$ is the number of data points. Because the scaling function/wavelet bases are made up of translations and dilations of their parent functions, the multiresolution decomposition is carried out only using the expansion and wavelet coefficients a_i^j and d_i^j. Starting with the initial expansion coefficients a_i^0, the a^j's are calculated at each scale from those of previous level [6]. The number of wavelet (and expansion) coefficients is halved as the resolution goes from fine to coarse ($j \rightarrow -m$) scales. The process ends with a single expansion coefficient as the coarsest approximation. It is by analyzing the distribution of the wavelet coefficients in the time-scale plane that information about the function can be deduced.

The signal can be reconstructed by the inverse wavelet transform which involves summing up the last expansion coefficient and all the wavelet coefficients.

In this paper we will refer to a particular scale (or level) by the value $|j|$ since the finest resolution is for $j = 0$, and the decomposition has $j = 0, -1, \ldots, -m$.

3 Application of wavelet theory

In applying wavelet theory to JINDALEE HF radar data, a number of considerations need to be addressed.

(i) Wavelet decomposition is traditionally performed on real valued functions; our data is in complex form. However, since the wavelet transform is a linear operator, the mathematical operations readily extend to complex valued functions. For our analysis we choose from the first ten Daubechies wavelets [7]. When applied to the data, complex wavelet coefficients are produced which can be viewed in both complex and polar representations.

(ii) A multiresolution wavelet decomposition begins with the initial expansion coefficients a_i^0 which correspond to the first approximation (2^0 resolution) of the signal with respect to the scaling function. In general, these are the data samples. However, to be mathematically correct, the data can be pre-filtered by the scaling function to produce the transformation into the scaling domain [6, 9]. We allow both cases.

(iii) There exists the problem of how to decompose a beam of time series data. A beam is an azimuth cell of time series data which are arranged in adjacent ranges, i.e, a 2-dimensional time versus range image. Usually for an image, 2-dimensional wavelet decomposition is performed [5]. However, here we are considering the x-axis as a time series and do not want to suppose a similar correlation across ranges. The wavelet decomposition is therefore, only performed in the horizontal direction and repeated across each range.

(iv) The possible introduction of artificial components from the wavelet processing. Being measured data the start and end values of the time series, in general, do not match up smoothly. This introduces a discontinuity into the data when calculating the expansion and wavelet coefficients since a periodicity condition is imposed. Having to work with relatively small data sets of 128 or 256 sample points, the spread of the resulting transient through the scales encroaches on a good part of the signal. Therefore, the data is initially extended on either side up to the next power of 2. This is where the time localization of the wavelet is an important property; for unlike the Fourier analysis, the inclusion of extra data will not corrupt the time-

scale (frequency) distribution of the true signal. The wavelet decomposition is performed on the extended data, but only the original time interval is displayed.

4 Wavelet domain filters

4.1 Thresholding wavelet coefficients

In the wavelet domain, we want to identify and reduce the contribution of transient signals in the data. We propose two methods to achieve this aim.

One method is to lower the magnitude of the wavelet coefficients which correspond to these signals. Figure 1 is a display of a multiresolution wavelet decomposition of a single, 128 point, complex time series using a Daubechies 8 wavelet. The two plots depict the magnitude of the real and imaginary wavelet coefficients in the time-scale plane starting from the finest detail d_i^{-1} at resolution 1/2 (scale 1) to the coarsest detail d_i^{-7} at resolution 1/128 (scale 7). The two colours indicate positive or negative values. As plotted, each scale has been normalized with respect to its maximum value. In reality, the magnitude of the coefficients at the coarsest scales (top) are much larger than those in the finest, hence the data is dominated by low frequency signals. The meteor information is characterized by a group of time localized peaks in the finest two scales. It is well separated from the strong ground clutter in the coarse scales ('low frequencies'), and stands out from the background noise in the finest scale ('high frequencies') during its brief existence.

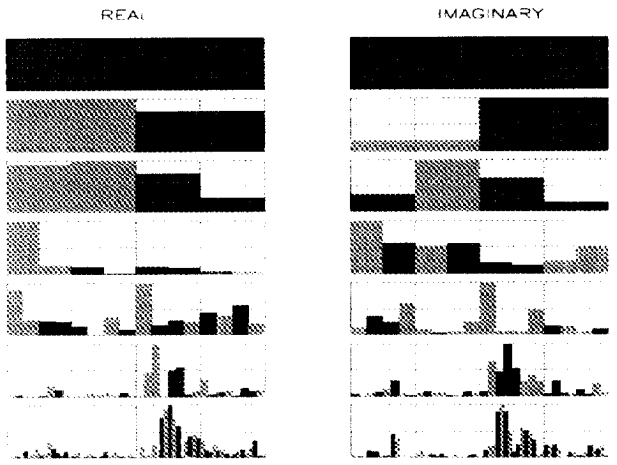

Figure 1: Daubechies 8 wavelet decomposition (time Vs scale) of complex time series data containing a meteor.

The meteor component is removed by a thresholding 'filter' which simply involves reducing the coefficients in each scale to a value chosen as a percentage of the maximum coefficient. Figure 2 illustrates the result of applying the filter to the finest two scales in the wavelet decomposition. The top plot is of the original time series data. The middle plot is of the reconstructed data after the coefficients in scales 1 and 2 had been reduced to 10 percent of the maximum coefficient. The bottom plot displays the difference between the two which is identified as the meteor signal. By only applying the filter to two scales we have avoided any interference to signals in the other frequency bands, e.g, clutter.

This procedure is opposite to the more traditional compression routines which involve removing small coefficients (over all scales) below a threshold value. Their aim is to 'clean up' the image and retain the majority of the information via the least number of coefficients. These coefficients tend to be the largest and often represent transients or edges in the image/signal. Our data contains large wavelet coefficients in the coarse scales due to the dominant ground clutter returns, so such a approach would retain mostly clutter signals.

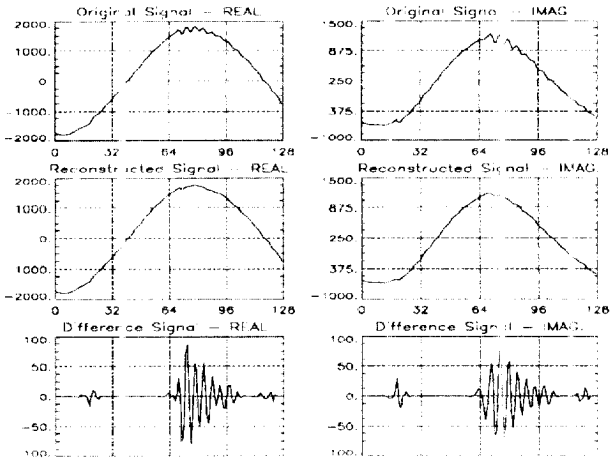

Figure 2: Coefficients in scales 1 and 2 of Figure 1. are thresholded to suppress the meteor components in the original data(top) then reconstructed (middle). The bottom graph is the extracted meteor component.

For this data there was no target present. If there had been, the filter might have removed the target first (see next section). Therefore, scales in which a target is present should not be filtered by this method.

4.2 Peak detection and suppression

Figure 3 is a display of the wavelet decomposition of a beam of time series data comprising of 20 ranges. The first four scales $\{\underline{d}^{-1}, \underline{d}^{-2}, \underline{d}^{-3}, \underline{d}^{-4}\}$ are illustrated with the finest scale plotted at the bottom right. The colour range is from the minimum to the maximum (white) absolute value in each scale. The data was processed by a Daubechies 6 wavelet. A high frequency target can be seen in scale 1 of the wavelet decomposition, and is in fact confined to this level. Targets exist for the full observation time (coherent integration time), and hence have small Doppler spread. In contrast, transients exist for short times and have large Doppler spread. The lightning produces vertical streaks over ranges in scales 1, 2 and 3. The thresholding filter cannot be used in scale 1 because the lightning components are smaller than that of the target. The excision technique needs to avoid the removal

of target information when detecting and suppressing transient coefficients.

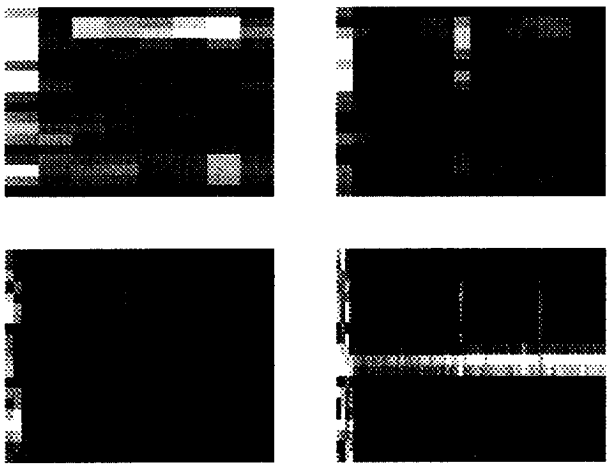

Figure 3: Time-range-scale distribution of a beam using a Daubechies 6 wavelet. A target is seen in the finest scale and lightning in the finest 3.

A second, more sophisticated algorithm incorporates a peak detector followed by amplitude suppression. For a chosen scale the arithmetic mean for each range over all times is calculated. Any wavelet coefficient whose amplitude is greater than 3dB of the average is not included in the calculation of the revised average value. All wavelet coefficients with amplitudes greater than 3dB of this new average are thresholded down to this value. The process detects and suppresses peaks in the time series while ignoring the target. This is because the target exists for the full coherent integration time, so it simply contribute to the background noise.

This method follows similar lines to that which is currently employed for transient detection [8]. The advantage of the implementation in the wavelet domain is that an initial clutter filter does not need to be applied in order to reveal the generally weaker impulsive noise; the wavelet decomposition effectively separates the high frequency bands from the low which contain the clutter. By thresholding the peaks via amplitude, the power associated with the transient is reduced such that it no longer interferes with target detection.

To remove the lightning from the data we run the peak detection and suppression routine over the three finest scales and reconstruct. Figure 4 illustrates the result of this filter on three adjacent beams. The top two images are the time and Doppler representations of the original data, where the lightning can be seen in the time domain as vertical streaks over all ranges and beams. The bottom two images are of the data after wavelet processing, lightning suppression and reconstruction. For plotting purposes a first difference filter was applied for the time plot and a Blackman-Harris window was used on the data before Doppler processing. On comparison in the time domain, most of the lightning has been removed. This is also evident in the Doppler domain where horizontal streaks (due to the spread in Doppler of the lightning) have been reduced. The target which shows up as a peak at high Doppler in the top two beams, has not been removed by the suppression process.

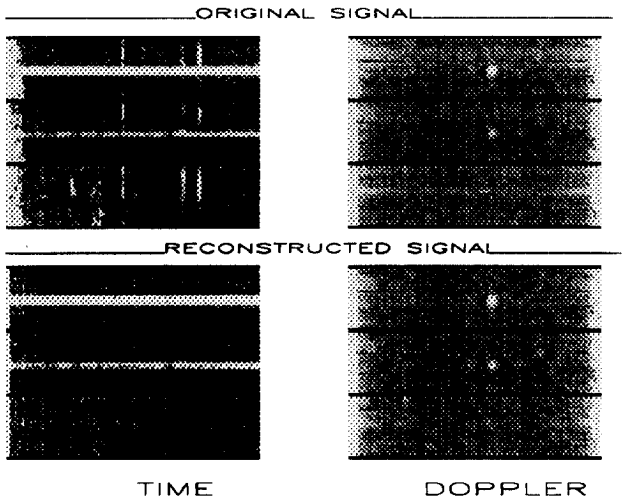

Figure 4: Azimuth-range-time and azimuth-range-Doppler plots of the original (top) and lightning suppressed (bottom) data. The suppression filter was applied to scales 1, 2 and 3 of each of the three beams.

Figure 5 is a display of the wavelet decomposition of a beam of time series data which contains a meteor echo. The data was decomposed by a Daubechies 6 wavelet. The peak detection and suppression filter is run on scales 1,2 and 3. The filter is not applied to scales greater than four (less than eight wavelet coefficients), since the time localization is too low to discern between a transient and a target, and above all, targets should not be removed.

Figure 6 illustrates the result of this filter on three adjacent beams which contain meteor echoes. The meteor is seen in the Doppler plot as a short, bright streak from medium to low negative frequencies. In the reconstructed data, the meteor echo has been reduced. However, not all of it has been removed. This could be due to the amplitude cutoff not being severe enough in the filtering process or the components of the meteor echo existing at the coarser scales which were not filtered.

5 Conclusion

We have performed a wavelet decomposition of OTH radar data and demonstrated two techniques designed to remove transient signals.

For this initial investigation we combined the traditional Daubechies wavelets with a standard multiresolution wavelet decomposition process modified to describe complex-valued, OTH radar data. The resulting time-scale distributions provided an informative representation of the time-series data. The separation of the frequency components allowed weak signals which are usually dominated by the low frequency

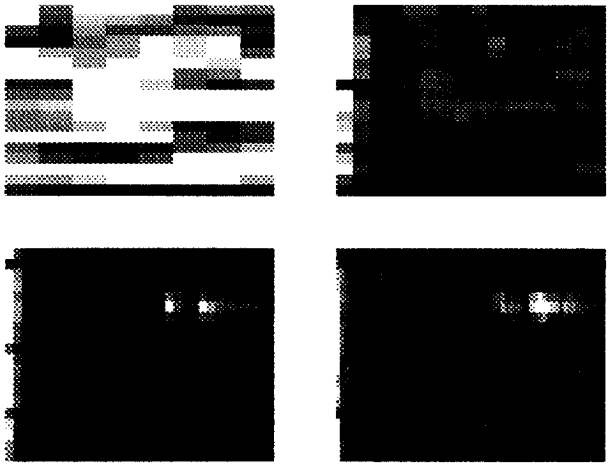

Figure 5: Time-range-scale distribution of a beam using a Daubechies 6 wavelet. A meteor echo contains components in the finest three scales.

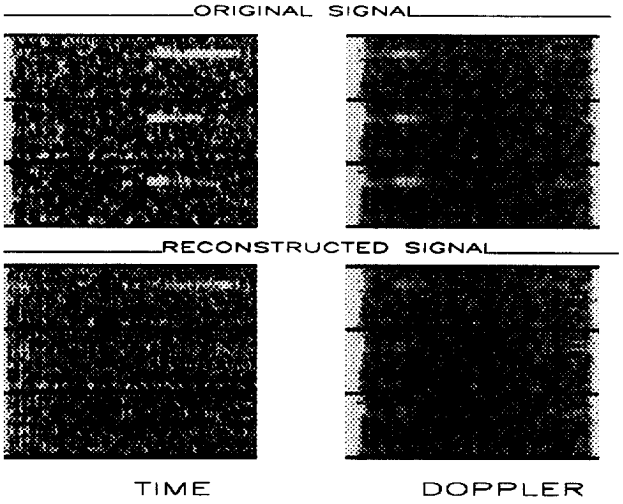

Figure 6: Azimuth-range-time and azimuth-range-Doppler plots of the original (top) and meteor suppressed (bottom) data. The transient suppressing filter was applied to scales 1,2 and 3 of each of the three beams.

clutter returns, to be revealed.

Two wavelet filtering techniques were applied to OTH radar data which contained lightning and meteor echoes. By implementing the filtering on individual scales in the wavelet domain the process was restricted in frequency as well as time, thus the removal of transients, although not always complete, caused less disruption to the non-transient information than the standard excision technique. Improvements to this process could be achieved through a better choice of wavelet, the use of higher multiplicity wavelets or the expansion into a wavelet packet algorithm [10].

We are currently exploring the construction of an optimal wavelet [11, 12] for our data. The aim is to match the wavelet to the unwanted transient signal so that it can be removed by eliminating a single scale subspace from the time-scale distribution.

Acknowledgements

The author would like to thank Dr C. Coleman, Mr C. Harlow, Dr S. Anderson and Dr J. Praschifka for their comments and suggestions.

References

[1] Netherway, D.J. and Ayliffe, J.K., 'Impulsive Noise Suppression in HF Radar', Digest of Papers, IREECON, Sydney, 1987

[2] Netherway, D.J., Ewing, G.E. and Anderson, S.J., 'Reduction of Some Environmental Effects that Degrade the Performance of HF Skywave Radars', *Proc.IEEE Aust. Conference on Signal Processing and Applications*, Adelaide, pp.288-292, April 1989

[3] Turley, M.D.E. and Netherway, D.J., 'OTHR Signal Reconstruction for Data Corrupted by Impulsive Noise', *Proceedings of Radarcon-90*, Adelaide, Australia, pp.203-209, April 1990

[4] Mallat, S.G., 'A Theory for Multiresolution Signal Decomposition: The Wavelet Representation', 1989, *IEEE Trans. Pattern Anal. Machine Intell.*, **11(7)**, 674–693.

[5] Mallat, S.G., 'Multiresolution Approximations and Wavelet Orthonormal Bases of $L^2(R)$', 1989, *Trans. Amer. Math. Soc.*, **315(1)**, 69–87.

[6] Coleman, C.J., 'An Implementation of Wavelet Analysis', *Technical Report SRL-0122-TR (1993)*, DSTO, Salisbury, South Australia.

[7] I. Daubechies., 'Ten Lectures on Wavelets', *CBMS-NSF 61 Series in Applied Mathematics, SIAM* 1992

[8] Lomen, J. and Praschifka, 'Interim Report on Assessment of Meteor Excision Algorithms (Air and Surface)', in preparation.

[9] Abry, P. and Flandrin, P., 'On the Initialization of the Discrete Wavelet Transform Algorithm', 1994, *IEEE Signal Proc. Letters*, **1(2)**, 32–34.

[10] Wickerhauser, M.V., 'Acoustic Signal Compression with Wavelet Packets' in *Wavelets: A Tutorial in Theory and Applications*, Ed. C.K.Chui., 1992 *Academic Press*, 679–700.

[11] Gopinath, R.A., Odegard, J.E. and Burrus, C.S., 'Optimal Wavelet Representation of Signals and the Wavelet Sampling Theorem', 1994, *IEEE Trans. Circuits and Systems—II: Analog and Digital Sig. Processing*, **41(4)**, 261–277.

[12] Tewfik, A.H., Sinha, D. and Jorgensen, P., 'On the Optimal Choice of a Wavelet for Signal Representation', 1992, *IEEE Trans. Inform. Theory*, **38(2)**, 747–765.